

Protein corona determines the cytotoxicity of nanodiamonds: implications of corona formation and its remodelling on nanodiamond applications in biomedical imaging and drug delivery

Dipesh Khanal^{1#}, Qingyu Lei^{1#}, Gabriela Pinget³, Daniel A. Cheong², Archana Gautam⁴, Ridhwan Yusoff⁴, Herman Hau⁴, Seiji Yamaguchi⁶, Alexey Kondyurin⁷, Jonathan C. Knowles^{8,9,10}, George Georgiou⁸, Laurence Macia³, Jun-Hyeog Jang¹¹, Iqbal Ramzan⁵, Kee Woei Ng^{4,12,13*}, Wojciech Chrzanowski^{1*}

*Correspondence: KWNG@ntu.edu.sg, wojciech.chrzanowski@sydney.edu.au

Physicochemical characterisation of the nanodiamond

Analysis of the aminated and pristine nanodiamonds revealed differences in their chemical properties. Low-resolution (bulk) chemical analysis (ATR-FTIR) of both classes of nanodiamond revealed main peaks at 1177 cm^{-1} , and 1256 cm^{-1} (**Fig. 1c**), which are associated with the stretching vibration of a C–O group and are characteristic of nanodiamonds.¹ For the aminated nanodiamonds (**red spectra, Fig. 1c**) an additional high intensity peak at 1660 cm^{-1} was observed, correlating to the bending N–H vibration associated with amides. Furthermore, a peak at 1630 cm^{-1} was present for both samples, associated with either bending mode of O–H or N–H. However, the intensity of this peak was much higher for the aminated nanodiamonds (**blue spectra, Fig. 1c**), which confirmed the presence of an N–H group in the aminated nanodiamonds². Additionally, peaks at 2280 cm^{-1} and 2350 cm^{-1} were observed only for the aminated nanodiamonds. These peaks may indicate the presence of nitrile groups, further confirming the successful amination of the nanodiamond surface³.

Finally, the peaks at 3400 cm^{-1} for both nanodiamond samples is associated with moisture bound to the nanodiamond surface.⁴ The results of the elemental analysis using XPS (**Fig. 1d, 1e**) also highlight the difference in chemistry between the aminated and pristine nanodiamond. Deconvolution of the high-resolution carbon (C 1s) spectra for the pristine nanodiamond showed three characteristic peaks at $E_B = 283.95\text{ eV}$, $E_B = 284.96\text{ eV}$ and $E_B = 286.23\text{ eV}$ (**Fig. 1e**) which corresponded to hybridized sp² carbon, hybridized sp³ carbon (diamond) and oxygen-containing groups (C–O) respectively. Similarly, three main peaks at $E_B = 285.2\text{ eV}$, $E_B = 284.35\text{ eV}$ and $E_B = 287.12\text{ eV}$ (**Fig. 1d**) that corresponded to sp², sp³ and C–O respectively were observed for aminated nanodiamonds. Deconvolution of the oxygen (O 1s) peaks for both nanodiamonds revealed one dominant peak at $E_B = 532.9\text{ eV}$ (pristine

nanodiamonds) and $E_B = 531.1$ eV (aminated nanodiamonds) associated with C–O–C and water adsorbed to the surface. Additionally, nitrogen (1.7%) was detected on the surface of the pristine nanodiamond. Nitrogen spectra for pristine nanodiamonds had two main peaks that correspond to N–C ($E_B = 400.6$ eV) and N_2 ($E_B = 404.1$ eV). Nitrogen spectra of aminated nanodiamonds showed two main peaks that correspond to NH_3 ($E_B = 398.8$ eV) and NH_4^+ ($E_B = 401.97$ eV).

The presence of functional groups on aminated nanodiamonds was confirmed by the differences in zeta potential (**Fig. 2b, c**). The aminated nanodiamonds were positively charged with a zeta potential ~ 20 mV. The pristine nanodiamonds were negatively charged with a zeta potential of -8 mV.

TEM and AFM images of both aminated (**Fig. 1a**) and pristine nanodiamonds (**Fig. 1b**) showed that individual nanodiamond particles had an average diameter of 4–5 nm. However, nanodiamond particles appeared mostly as agglomerates with an average diameter of 200 nm. Nanoparticle tracking analysis (NTA) results confirmed the tendency of nanodiamond to agglomerate. Moreover, the size of agglomerates ranged from 22–233 nm for pristine nanodiamond and 10–211 nm for aminated nanodiamonds (**Fig. 2a**). Agglomeration may have occurred due to the formation of dangling bonds on nanodiamond surfaces during nanodiamond manufacturing.⁵ The presence of free electrons on the surfaces of nanodiamond make them highly reactive and may result in the formation of surface bound functional groups such as hydroxyl or carboxyl. Chemically reactive groups on primary particle surfaces may encourage intraparticle interactions, leading to the formation of covalent bonds and causing agglomeration.^{5–7} Furthermore, the abundance of van der Waals forces, dipole–dipole interactions, hydrogen bonding and electrostatic forces also enables strongly-bound nanodiamond agglomerates to form.

XRD analysis for both variants of nanodiamond showed two maxima at 2θ of 43.9 and 75.4 (**Fig. 1f**) which correspond to diamond peaks.⁸ The average grain size of the crystals for both nanodiamond were estimated to be 5 nm using the Scherrer formula (**Fig. 1f**), which agreed with TEM and AFM results (**Fig. 1a, b**). The surface areas were estimated to be 222.5 m² g⁻¹ for aminated nanodiamond and 195.9 m² g⁻¹ for pristine nanodiamond using the BET equation.

Figure S1.

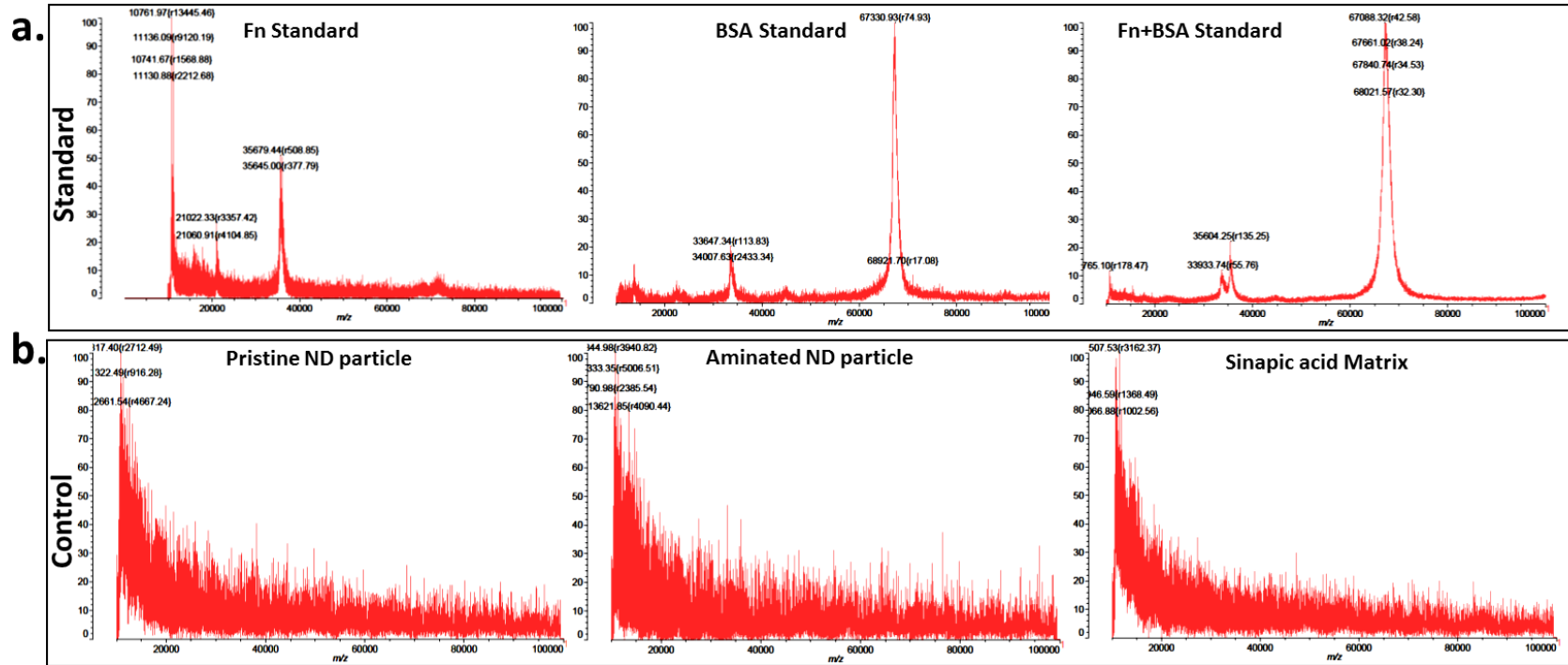


Fig. S1: MALDI-TOF spectra collected from control samples. (a) From left to right spectra collected from Fn standard, BSA standard and mixture of Fn and BSA. Individual spectra present distinct peaks for the proteins. However, when mixed, BSA overpowers Fn spectra; (b) Spectra acquired from control particle and matrix used for measurement.

Figure S2.

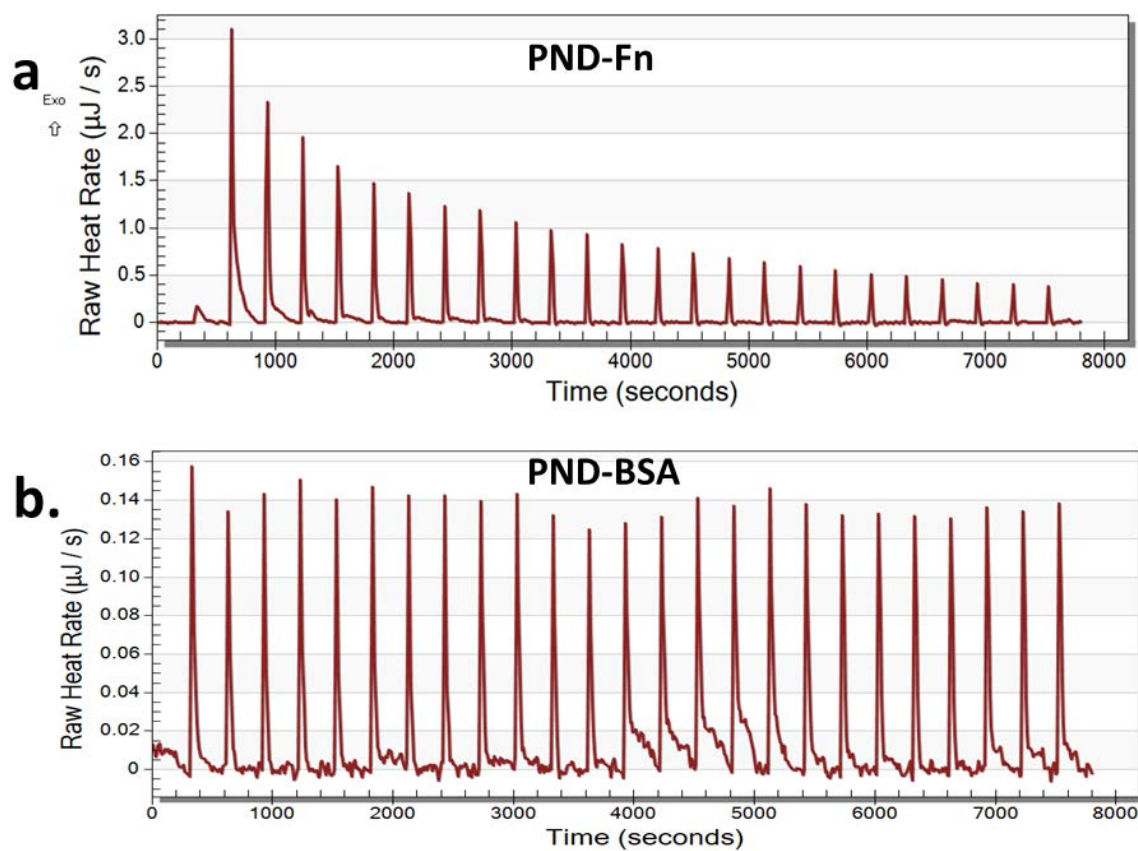


Fig.S2: Isothermal calorimetry plot of Fn and BSA titrated with pristine nanodiamonds. (a) Binding of Fn to nanodiamonds is an exothermic process and with increased number of injection of Fn, heat release associated to binding of protein decreased and after 2h equilibrium state was reached indicating the possible saturation of binding domains present on nanodiamonds surface; (b) Binding of BSA to nanodiamonds was also an exothermic process, however the amount of heat release after binding to nanodiamonds was lower than the heat release during Fn titration. This indicated lower affinity of BSA to aminated nanodiamonds.

Figure S3.

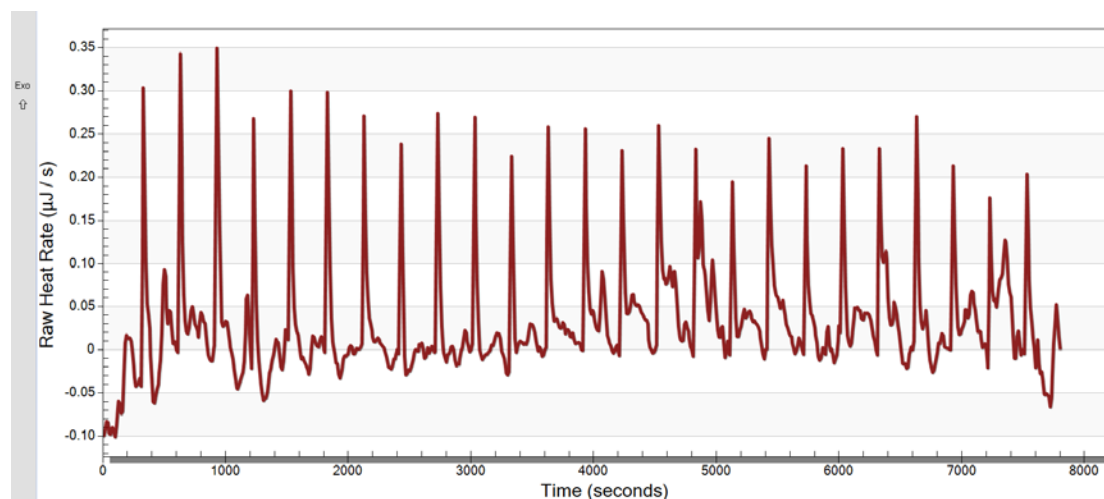


Fig.S3: Isothermal calorimetry plot of BSA titrated with pristine nanodiamonds, erratic isotherm peaks were observed possibly due to the instability of particles or tendency of particles to aggregate or proteins to aggregate in presence of nanoparticles.

REFERENCES

1. M. V. Baidakova, Y. A. Kukushkina, A. A. Sitnikova, M. A. Yagovkina, D. A. Kirilenko, V. V. Sokolov, M. S. Shestakov, A. Y. Vul', B. Zousman and O. Levinson, *Physics of the Solid State*, 2013, **55**, 1747-1753.
2. V. N. Mochalin, I. Neitzel, B. J. Etzold, A. Peterson, G. Palmese and Y. Gogotsi, *ACS nano*, 2011, **5**, 7494-7502.
3. G. Jarre, S. Heyer, E. Memmel, T. Meinhardt and A. Krueger, *Beilstein journal of organic chemistry*, 2014, **10**, 2729.
4. D. Khanal, A. Kondyurin, H. Hau, J. C. Knowles, O. Levinson, I. Ramzan, D. Fu, C. Marcott and W. Chrzanowski, *Analytical Chemistry*, 2016, **88**, 7530-7538.
5. A. Pentecost, S. Gour, V. Mochalin, I. Knoke and Y. Gogotsi, *ACS applied materials & interfaces*, 2010, **2**, 3289-3294.
6. A. Krüger, Y. Liang, G. Jarre and J. Stegk, *Journal of Materials Chemistry*, 2006, **16**, 2322-2328.
7. A. S. Barnard, *Journal of Materials Chemistry*, 2008, **18**, 4038-4041.
8. B. D. Holt, P. A. Short, A. D. Rape, Y.-l. Wang, M. F. Islam and K. N. Dahl, *ACS Nano*, 2010, **4**, 4872-4878.